Acta Crystallographica Section B
Structural Science
ISSN 0108-7681

Klockmannite, CuSe: structure, properties and phase stability from *ab initio* modeling

Victor Milman

Accelrys, The Quorum, Barnwell Road, Cambridge CB5 8RE, England

Correspondence e-mail: vmilman@accelrys.com

Received 29 September 2001
Accepted 18 February 2002

The details of the electronic and crystal structure, the nature of the interatomic bonding and the phase stability of three modifications of klockmannite, CuSe, are analysed using first principles modeling. The hexagonal modification of CuSe is predicted to be less stable than the orthorhombic phase under pressure. The stabilizing force for the orthorhombic phase is identified as the Cu—Cu bond formation between the Cu atoms in the flat hexagonal CuSe layer and in the buckled Cu_2Se_2 layer. Furthermore, klockmannite is shown to be unstable under compression with respect to the decomposition into umangite, Cu_3Se_2, and krutaite, $CuSe_2$ II.

1. Introduction

Experimental studies of the structure and phase diagram of the natural and synthetic mineral klockmannite, CuSe, have been reported as early as 1949 (Earley, 1949). The history of these investigations reveals a number of unresolved controversies and the recent high-pressure study of this mineral by Peiris *et al.* (1998) adds to the list of unexplained results. A review of the experimental and theoretical studies of klockmannite given below clearly shows that despite decades of research there are fundamental gaps in the understanding of this mineral and its properties, mainly because of the remarkable structural complexity of klockmannite.

The early studies by Earley (1949) and Berry (1954) identified synthetic klockmannite as isostructural with covellite, CuS. This hexagonal modification of CuSe crystallizes in the $P6_3/mmc$ space group ($Z = 6$), with two Cu1 atoms on 2(*d*) Wyckoff sites (1/3, 2/3, 3/4), four Cu2 atoms on 4(*f*) sites (1/3, 2/3, Cu_z), two Se1 atoms on 2(*c*) sites (1/3, 2/3, 1/4) and four Se2 atoms on 4(*e*) sites (0, 0, Se_z). Cu1 atoms are coordinated to three Se1 atoms in the (0001) plane, while Cu2 is surrounded by three Se2 atoms and one Se1 atom in a nearly perfect tetrahedral coordination, see Fig. 1. The structural parameters available from experimental studies are given in Table 1. The structure can be described as alternating planar hexagonal layers, Cu1—Se1, and double layers of CuSe tetrahedra, Cu2—Se2. The Se_2 dumbbells link the tetrahedra within the double layer.

The ageing of klockmannite results in the appearance of the pronounced superstructure (Earley, 1949; Berry, 1954; Taylor

Table 1
Experimental and theoretical structure of hexagonal CuSe.

Experimental techniques are denoted as P (powder X-ray diffractometry), SC (single-crystal X-ray diffractometry) or PR (powder X-ray diffractometry with Rietveld refinement). α-CuSe is the low-temperature modification, whilst γ-CuSe is the high-temperature phase. The value quoted as a for α-CuSe represents $a'/(13)^{1/2}$, where a' is the actual cell parameter.

Phase	a (Å)	c (Å)	Cu_z	Se_z	V (Å^3)	T (K)	Comment
$\alpha^{(a)}$	3.93 (1)	17.22 (5)	–	–	230.3 (2.0)	293	P
$\alpha^{(b)}$	3.938	17.25	0.107	0.068	231.67	293	P
$\alpha^{(c)}$	3.954	17.25	–	–	233.56	293	P
$\alpha^{(d)}$	3.940 (3)	17.216 (5)	–	–	231.45 (50)	299	P
$\alpha^{(e)}$	3.938	17.26	–	–	231.81	293	P
$\alpha^{(f)}$	3.934	17.217	–	–	230.76	298	P
$\alpha^{(g)}$	3.939 (2)	17.25 (5)	–	–	231.8 (1.0)	293	SC
$\alpha^{(h)}$	3.94	17.25	–	–	231.91	293	SC
$\alpha^{(i)}$	3.9444 (17)	17.265 (7)	–	–	232.63 (15)	297	P
$\alpha^{(j)}$	3.938 (1)	17.255 (1)	–	–	231.74 (14)	293	PR
$\alpha^{(k)}$	3.975	17.355 (1)	–	–	237.52	0	–
$\gamma^{(e)}$	3.976	17.243	–	–	236.07	413	P
$\gamma^{(f)}$	3.984	17.288	–	–	237.64	430	P
$\gamma^{(i)}$	3.9887 (13)	17.244 (7)	–	–	237.59 (16)	407	P
$\gamma^{(j)}$	3.980 (1)	17.254 (1)	0.1089 (6)	0.0678 (7)	236.69 (14)	515	PR
$\gamma^{(j)}$	3.973	17.350	0.1076	0.0687	237.15	0	–

References: (*a*) Earley (1949); (*b*) Berry (1954); (*c*) Taylor & Underwood (1960); (*d*) Heyding (1966); (*e*) Stevels (1969) and Stevels & Jellinek (1971); (*f*) Murray & Heyding (1975); (*g*) Von Effenberger & Pertlik (1981); (*h*) Brun *et al.* (1982); (*i*) Nozaki *et al.* (1994); (*j*) Stølen *et al.* (1996); (*k*) present results.

& Underwood, 1960; Lippmann, 1962; Darlow, 1969; Elliott *et al.*, 1969). The observed pattern is commonly interpreted as being due to the twinning, so that the true hexagonal cell has $a' = a(13)^{1/2}$, $c' = c$ (Taylor & Underwood, 1960). This description corresponds to 78 CuSe formula units in a true cell. Lippmann (1962) suggested that the true cell had a lower symmetry, $P6_3/m$, and proposed a set of internal coordinates for this space group.

The driving force for the lowering of symmetry was explained by Lippmann (1962) based on the comparison of klockmannite to covellite, CuS, where hexagonal structure with $Z = 6$ remains stable on ageing. In the case of covellite the side length of the Cu2—S2 tetrahedron, 3.784 (1) Å, is fortuitously close to the side length of the S1—S1 equilateral triangle, 3.792 (1) Å (Fjellvåg *et al.*, 1988), with the mismatch of only 0.008 Å. The mismatch between the tetrahedron side length, 3.894 (1) Å, and the triangle side length, 3.980 (1) Å, is more noticeable (0.086 Å) in klockmannite (Stølen *et al.*, 1996). The lowering of the space-group symmetry allows a large fraction of Cu and Se atoms to be displaced from the special positions, thus locally reducing the tetrahedron-triangle mismatch by crimping the tetrahedral layer to match a flat hexagonal layer. This corrugated layered structure would have 26 parameters to be refined based on the experimental X-ray data, which appeared to be beyond the capabilities of experimental techniques (Lippmann, 1962).

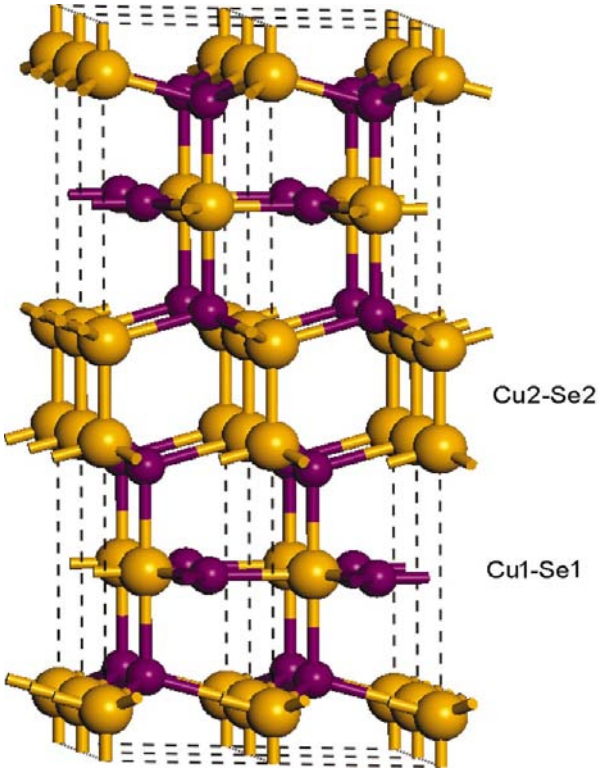

Figure 1
Layered structure of hexagonal CuSe (Cu: smaller spheres; Se: bigger spheres).

An alternative picture of the low-temperature modification was suggested by Von Effenberger & Pertlik (1981). They assumed the presence of the ordered tetrahedral layers, Cu2—Se2, alternating with the disordered Cu1—Se1 sheets. This corresponds to the description in which the atomic positions are statistically occupied, and the superlattice reflections are explained by the partial ordering of these sheets.

Klockmannite undergoes a series of transitions on heating, as was established by numerous studies (Heyding, 1966; Stevels, 1969; Stevels & Jellinek, 1971; Murray & Heyding, 1975; Brun *et al.*, 1982; Nozaki *et al.*, 1994). The most comprehensive and accurate experimental results on the thermodynamics of klockmannite are due to Stølen *et al.* (1996).

The hexagonal superstructure of α-CuSe on heating undergoes a rapid polymorphic transition to an orthorhombic structure, β-CuSe. The structural parameters of this modification are given in Table 2. The transition temperature of 327 K determined by Stølen *et al.* (1996) agrees well with the earlier results: 326 K (Heyding, 1966), 320 K (Stevels & Jellinek, 1971), 324 K (Murray & Heyding, 1975) and 323 K (Brun *et al.*, 1982; Nozaki *et al.*, 1994). The $\alpha \rightarrow \beta$ transformation is characterized as the first-order transition based on the analysis of the temperature dependence of transport properties (Brun *et al.*, 1982) and of the cell parameters (Brun

Table 2
Experimental and theoretical structure of orthorhombic CuSe.

a (Å)	b (Å)	c (Å)	$V/2$ (Å^3)	$b/a3^{1/2}$	T (K)
4.01 (1)	6.81 (1)	17.09 (2)	233.3 (1.2)	0.980	336[(a)]
3.949	6.935	17.20	235.52	1.014	333[(b)]
3.948	6.958	17.239	236.78	1.017	324[(c)]
3.9472 (12)	6.9601 (44)	17.244 (6)	236.9 (5)	1.018	325[(d)]
3.952 (1)	6.962 (1)	17.235 (1)	237.1 (1)	1.017	353[(e)]
3.954 (1)	6.911 (1)	17.304 (1)	236.4 (1)	1.009	0[(f)]

References: (*a*) Heyding (1966); (*b*) Stevels (1969); (*c*) Murray & Heyding (1975); (*d*) Nozaki *et al.* (1994); (*e*) Stølen *et al.* (1996) (*f*) present results.

et al., 1982; Nozaki *et al.*, 1994; Stølen *et al.*, 1996). The $\alpha \rightarrow \beta$ transformation enthalpy, $\Delta H_{\alpha \rightarrow \beta}$, is reported as 1.38 (38) kJ mol^{-1} (Heyding, 1966), 0.84 kJ mol^{-1} (Murray & Heyding, 1975) and 0.8553 (2) kJ mol^{-1} (Stølen *et al.*, 1996). These values are exceedingly small by the standards of atomistic modeling, so it is a computational challenge to achieve the accuracy necessary to reproduce the energy difference of this magnitude.

Further heating of the orthorhombic β-CuSe causes a sluggish second-order transition to another hexagonal modification, γ-CuSe, at 410 K (Stølen *et al.*, 1996). Other reported values of the transition temperature are 393 K (Stevels, 1969; Stevels & Jellinek, 1971; Murray & Heyding, 1975), 373 K (Brun *et al.*, 1982) and 398 K (Nozaki *et al.*, 1994). The change in c parameter is very small on both transitions and the main effect is the splitting of the hexagonal parameter a into a and $b/3^{1/2}$ in the orthorhombic structure. The cell volume changes discontinuously in the $\alpha \rightarrow \beta$ transition and continuously in the $\beta \rightarrow \gamma$ transition (Nozaki *et al.*, 1994; Stølen *et al.*, 1996).

The basic picture of three distinct CuSe modifications is incomplete without considering metastable polymorphs (Nozaki *et al.*, 1994) and pressure-induced transitions. It was shown, for example, that α-CuSe disproportionates into umangite, Cu_3Se_2, and krutaite, $CuSe_2$ II, at a pressure of $\sim$1 GPa (Murray & Heyding, 1975). Disproportionation occurs at even lower pressures of 0.3–0.5 GPa after non-hydrostatic deformation *via* grinding.

A detailed study of the temperature dependence of the interatomic bond lengths in klockmannite shows that the orthorhombic distortion of the hexagonal γ -CuSe structure is likely to be driven by the shortening of the Cu1—Cu2 distances, and to a lesser extent by the shortening of the Se1—Se2 distances (Stølen *et al.*, 1996). The Cu1—Cu2 separation decreases from 3.35 to 3.20 Å upon cooling through the $\gamma \rightarrow \beta$ transition point. This value becomes closer to *e.g.* the Cu—Cu bond length in metallic copper, 2.56 Å, which indicates the possibility of the creation of a proper bond between the two Cu atoms. A similar hypothesis has been put forward for the isostructural mineral covellite, CuS, that exhibits a second-order phase transition at 55 K from the high-temperature hexagonal modification to the low-temperature orthorhombic phase. The distortion is similar to the one observed in the $\gamma \Rightarrow \beta$ transition in CuSe and has been explained by the bond formation between Cu1 and Cu2 atoms (Fjellvåg *et al.*, 1988).

The effect of cooling on the structure and properties of solids is often similar to that of applying external pressure. One can therefore expect a variety of pressure-induced transitions in klockmannite. The structure of CuSe under compression has been studied by Peiris *et al.* (1998). The X-ray diffraction spectra were indexed using the hexagonal cell description up to 52 GPa, despite the presence of three strong peaks that could not be assigned to either the CuSe lattice or to superlattice reflections. A number of peaks lost intensity under compression, which Peiris *et al.* (1998) explained as a possible '*minor phase change*'. Raman peaks also showed splitting and/or a drastic decrease in intensity upon compression, which indicated that the phase transition under pressure could not be ruled out.

The bulk modulus $B = 96.9 \pm 5.3$ GPa and its pressure derivative $B' = 4.14 \pm 0.47$ were determined by Peiris *et al.* (1998) from the fit with a third-order Birch–Murnaghan equation of state (Birch, 1978). The statistical error of the fit is quite large as a result of large error bars on the experimental data points and it will be shown in this paper that the values obtained by Peiris *et al.* (1998) are probably unreliable.

The high-pressure study by Peiris *et al.* (1998) is in open contradiction with the earlier results on the phase stability of CuSe. Klockmannite disproportionation was previously reported at a pressure as low as 1 GPa (Murray & Heyding, 1975), thus it is surprising that no clear sign of phase transition was observed by Peiris *et al.* (1998) up to 52 GPa.

The present study applies the first principles quantum-mechanical description to investigate the stability of various modifications of CuSe under pressure, including the low-temperature structure of klockmannite with 78 formula units per cell. The aim of the study was to gain insight into the driving forces of the orthorhombic distortion of the covellite structure, as well as to predict the structural and electronic changes in CuSe under pressure.

2. Computational details

The quantum mechanical calculations performed here are based on density functional theory, DFT (Hohenberg & Kohn, 1964; Kohn & Sham, 1965). Exchange-correlation effects were taken into account using the Perdew–Wang generalized gradient correction functional, GGA (Perdew *et al.*, 1992), as implemented by White & Bird (1994). The total energy code *CASTEP* was used (Payne *et al.*, 1992; Milman *et al.*, 2000; Accelrys Inc., 2001), which utilizes pseudopotentials to describe electron–ion interactions and uses plane-wave basis sets to represent wavefunctions. Ultrasoft pseudopotentials (Vanderbilt, 1990) were used with 11 and six valence electrons for Cu and Se, respectively. The energy cutoff of 340 eV was used for all the calculations. Monkhorst & Pack's (1976) special k-points technique was used to sample the Brillouin zone. All systems were treated as metallic by using partial occupation numbers for electron levels close to the Fermi energy (De Vita, 1992). The density mixing scheme was used for the self-consistent solution of the density functional equations (Kresse & Furthmüller, 1996). Geometry optimi-

zation, including both cell parameters and internal degrees of freedom, was performed using the BFGS technique (Fischer & Almlöf, 1992). Previous experience shows that this description of inorganic compounds produces interatomic distances within 1% of experimental values (Milman *et al.*, 2000).

The systems studied included the covellite-type hexagonal modification, γ-CuSe; orthorhombic modification, β-CuSe; krutaite, $CuSe_2$ II (cubic pyrite-type structure, space group $Pa\bar{3}$); umangite, Cu_3Se_2 (tetragonal, space group $P\bar{4}2_1m$); and finally the $(13)^{1/2}$ structure of α-CuSe (space group $P6_3/m$). Geometry optimization has been performed for all these compounds at $P = 0$ and under compression. The structural changes and modifications of the electronic structure as well as the energetic stability have been examined in order to identify the driving force for the orthorhombic distortion. The bulk modulus and its pressure derivative were obtained from fitting the calculated equation of state, EOS, using a third-order Birch–Murnaghan EOS (Birch, 1978).

Convergence testing has been performed for each system studied, by repeating the calculations with higher-energy cutoffs, up to 450 eV, and better *k*-point sets. The results were found to be converged to better than 0.001 Å for cell parameters and 0.0001 for fractional atomic coordinates.

3. Theoretical results

The results presented below refer to different modifications of CuSe with the symmetry being fixed to the experimentally observed one. A further set of results was obtained by reducing the symmetry of some of the structures to *P*1 and allowing complete structural relaxation under pressure.

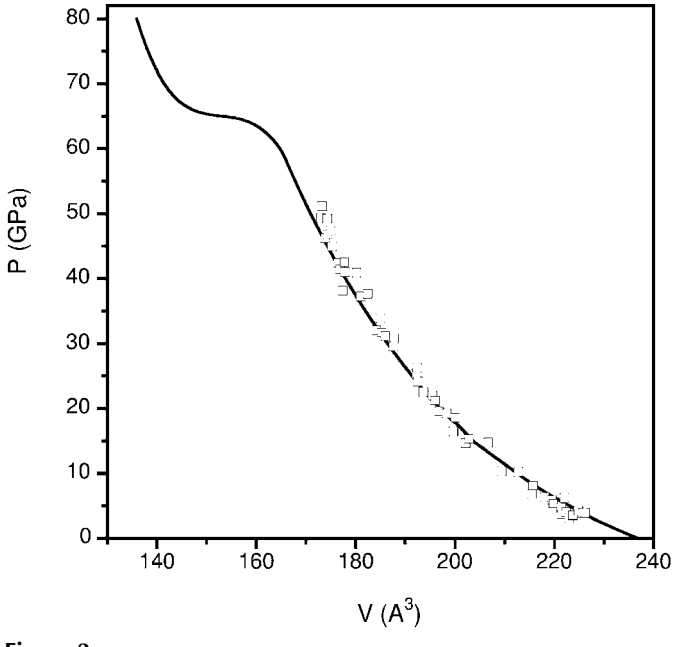

Figure 2
Equation of state of hexagonal CuSe. Squares: experiment (Peiris *et al.*, 1998); solid line: present results.

3.1. Hexagonal γ-CuSe

The calculated equation of state up to 80 GPa for the hexagonal CuSe modification is presented in Fig. 2, the equilibrium lattice parameters and internal coordinates of Cu and Se atoms are given in Table 1. The comparison with numerous experimental results for the high-temperature hexagonal modification of CuSe shows that the calculated structural parameters for the ground state are accurate to better than 0.2%. This agreement with experiment should not be affected by taking account of the thermal expansion. There are indications that the thermal expansion coefficient of γ-CuSe is very small and possibly even negative (Stølen *et al.*, 1996).

The bulk modulus and its pressure derivative were obtained from the theoretical data shown in Fig. 2 as 72 (1) GPa and 4.59 (7), respectively. The pressure range of 50 GPa was used in the fitting procedure, which is the same range as in the experimental study (Peiris *et al.*, 1998). The results were unchanged within the calculated uncertainty when the pressure range for the EOS fitting was reduced to 10 GPa, which indicates that the third-order Birch–Murnaghan equation accurately describes the compressibility of hexagonal CuSe.

It is not clear to what degree the structure of the low-temperature hexagonal phase is different from the high-temperature one. All the experimental data indicate that there

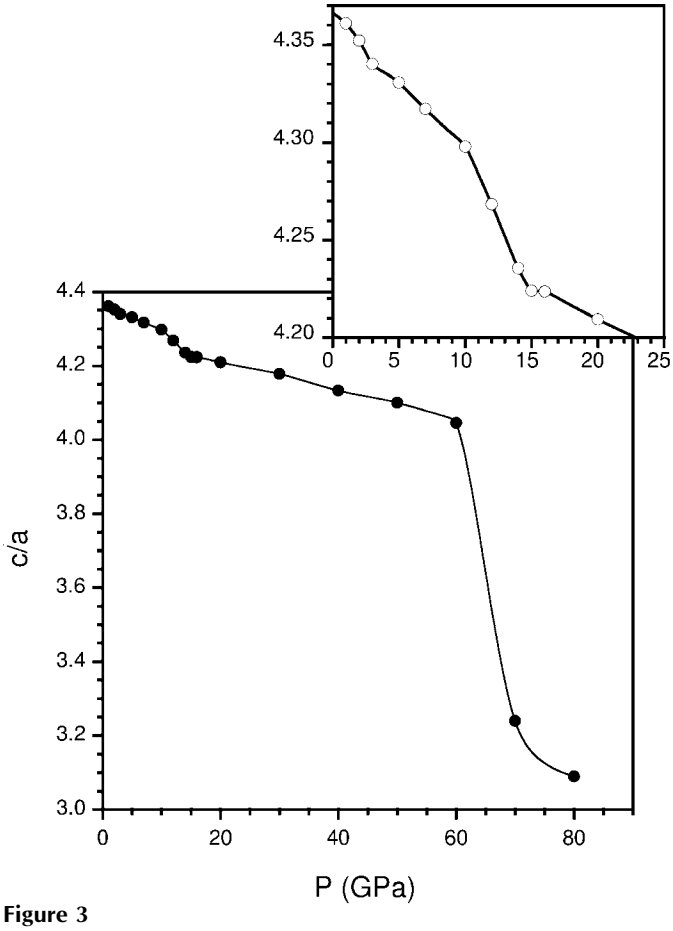

Figure 3
Pressure dependence of the *c*/*a* ratio for hexagonal CuSe. The insert shows low-pressure behaviour in more detail.

are only minor structural differences between the two modifications. It is thus legitimate to use γ-CuSe as the model structure to study the effect of pressure on hexagonal klockmannite. The equilibrium structure of CuSe in the space group $P6_3/mmc$ was examined in the range of pressures from zero to 80 GPa. Although this structure is not expected to remain stable under such pressures, the analysis can shed light on the nature of structural instabilities and point to precursors of pressure-induced phase transitions (Milman, 1997).

Analysis of the pressure dependence of the c/a ratio shows that the structure changes drastically at around 60 GPa (Fig. 3). The c/a ratio decreases from ~4 to 3 as a result of the rapid shortening of the c axis accompanied by a strong increase of the a axis. The anomaly at 60 GPa can also be seen on the P–V diagram, Fig. 2. The nature of the structural change is further illustrated by Figs. 4 and 5 that show the pressure dependence of the two internal degrees of freedom, Cu_z and Se_z, and of the selected interatomic distances. The Cu1—Cu2 distance drops dramatically above 60 GPa, from 3.4 to 2.25 Å. This change is achieved by the weakening of the Se–Se dumbbells and forming new bonds between the Se1 and Se2 atoms. This is accompanied by the movement of the Cu2 atoms through the corrugated sheets so that the value of Cu_z becomes negative above 60 GPa, see Fig. 4. As a result proper metallic bonds are

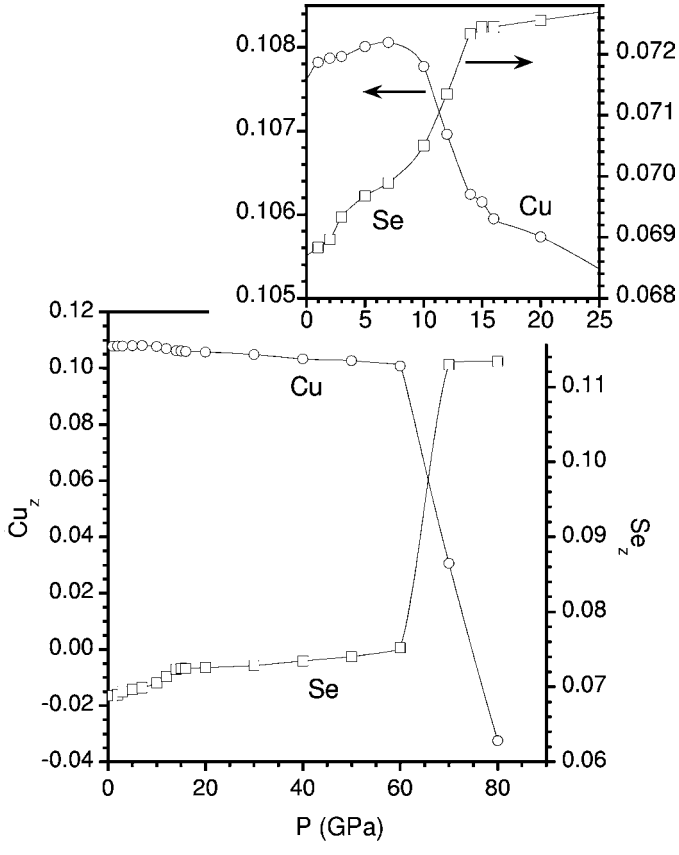

Figure 4
Pressure dependence of Cu_z and Se_z coordinates in hexagonal CuSe. The insert shows low-pressure behaviour in more detail.

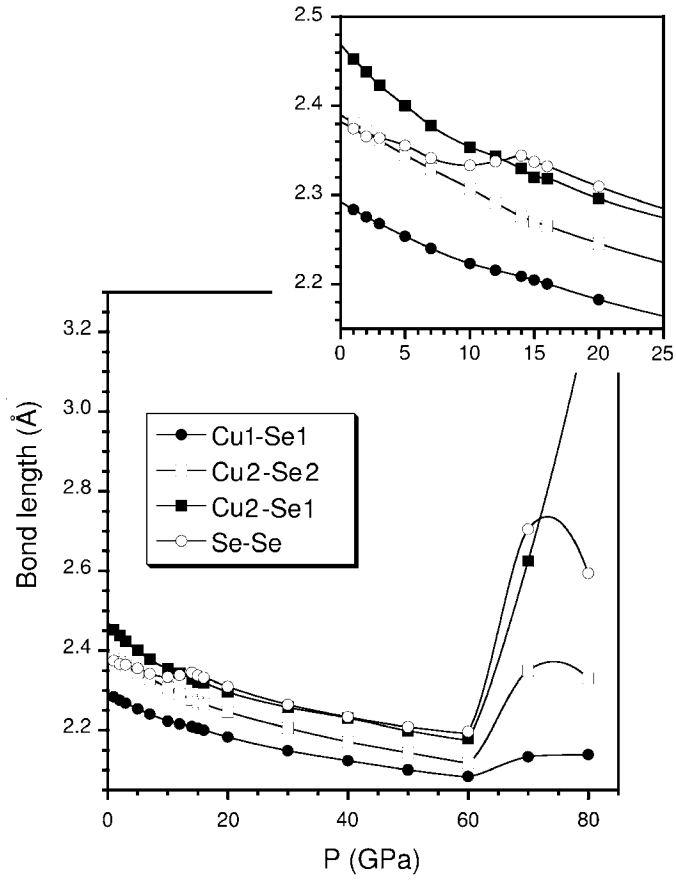

Figure 5
Pressure dependence of selected interatomic distances in hexagonal CuSe. The insert shows low-pressure behaviour in more detail.

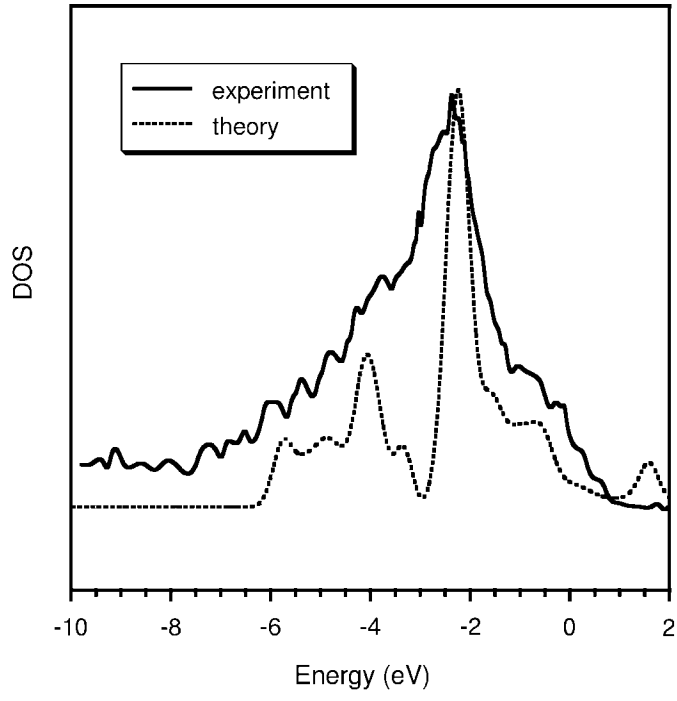

Figure 6
Experimental (Fowlmer & Jellinek, 1980; solid line) and calculated (dashed line) density of states of hexagonal klockmannite.

established between the Cu1 and Cu2 atoms, so that the structure can no longer be described as covellite.

The structural changes at 60 GPa are accompanied by the fundamental changes in the electronic structure of the material. Electronic properties of klockmannite were studied experimentally by Fowlmer & Jellinek (1980) using X-ray photoelectron spectroscopy, XPS. They described klockmannite as $Cu_3^+(Se_2)^{2-}Se^-$ to reflect the different nature of the Se atoms in the dumbbells from those in the hexagonal plane. The metallic character of klockmannite with *p*-type conductivity is ascribed to the holes in the Se(4*p*) band (Fowlmer & Jellinek (1980).

The comparison of the calculated density of states (DOS) with the experimental data of Fowlmer & Jellinek (1980) shows satisfactory qualitative agreement, Fig. 6, especially since the photoelectron spectra do not produce DOS directly. No matrix element effect was introduced in the present calculation, so that one can reliably compare only the position and not the intensity of the peaks in Fig. 6. The metallic character of klockmannite is reproduced in the calculation and can be seen as a non-zero density of states at the Fermi energy (zero energy in Fig. 6). The overall width of the valence band is roughly 6.5 eV, which is qualitatively consistent with the value of 7 eV obtained from the low-resolution spectra (Fowlmer & Jellinek, 1980). The Cu-3*d* peak is found 2.5 eV above the bottom of the valence band, in agreement with the experimental value of 3 eV (Fowlmer & Jellinek, 1980).

Applied pressure causes substantial widening and hybridization of electronic bands, as illustrated by Fig. 7. The valence band of hexagonal CuSe consists of two subbands separated by the internal band gap of approximately 0.4 eV at ambient conditions (Fig. 8). This band gap decreases under pressure and disappears at ~60 GPa. It is known that internal band gap closure can be related to structural instabilities (Winkler &

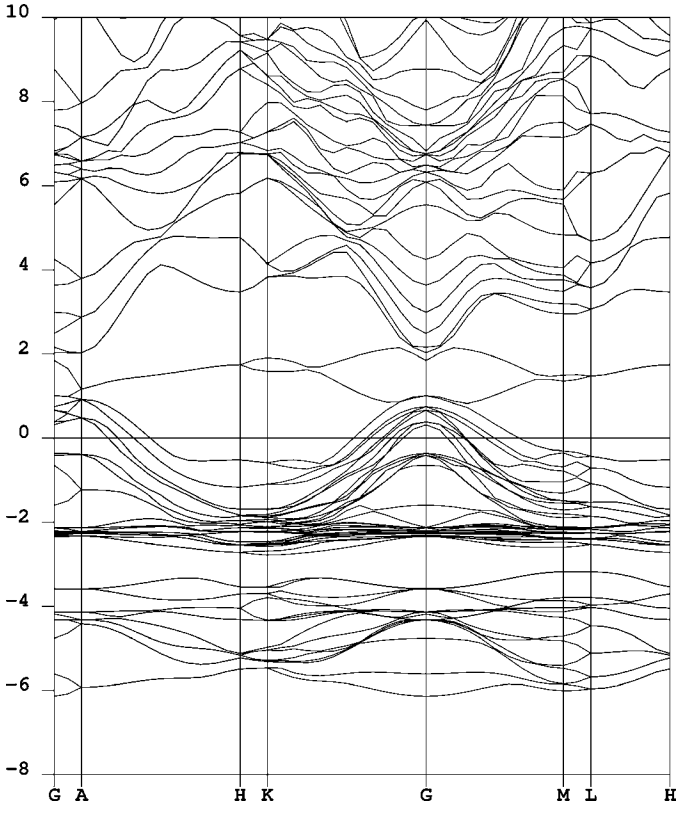

Figure 8
Band structure of hexagonal CuSe at ambient conditions (band energies in eV, Fermi level corresponds to zero energy).

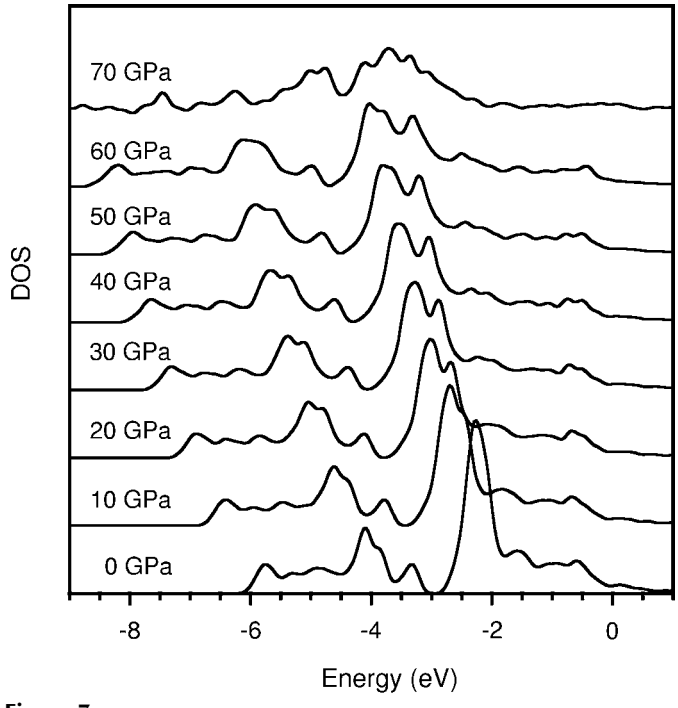

Figure 7
Pressure dependence of the electronic density of states of hexagonal CuSe.

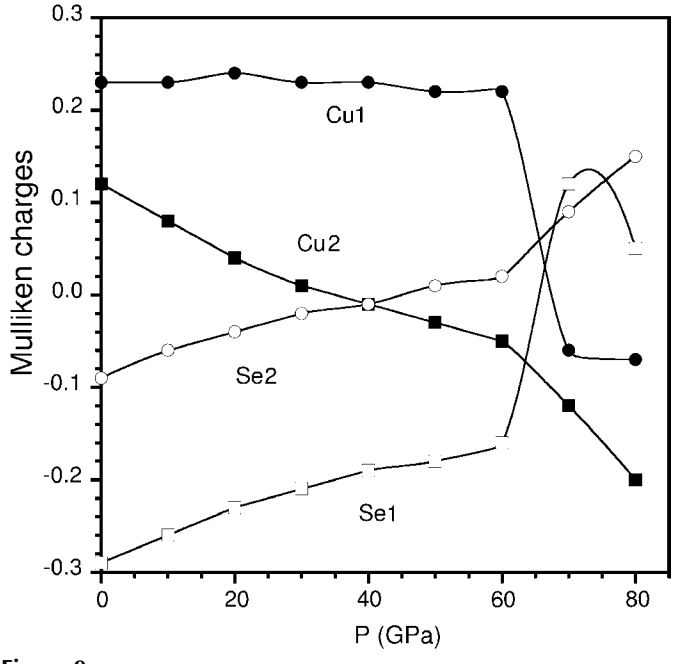

Figure 9
Pressure dependence of Mulliken charges on Cu and Se atoms in hexagonal CuSe.

Milman, 1997). This appears to be the case for hexagonal CuSe: the pressure which causes the closure of the band gap corresponds exactly to the occurrence of the drastic structural changes illustrated by Figs. 4–6.

The band structure at ambient pressure illustrated in Fig. 8 presents an interesting feature. The lower part of the valence band is separated by band gaps from both the semicore Se 4*s* states and from the upper part of the valence band which is responsible for the metallic character of CuSe. The unit cell of CuSe used in the calculations contains six Cu atoms with the nominal electronic configuration of $3d^{10}4s^{1}$ and six Se atoms with the configuration $4s^{2}4p^{4}$. The semicore Se 4*s* electrons form three fully occupied bands carrying four electrons each and thus do not contribute to the lower valence band. If all *d* electrons of Cu atoms were localized in the upper valence band, there would be six Cu 4*s* electrons and 24 Se 4*p* electrons, 30 electrons altogether. However, the lower valence band contains 32 electrons. This can be explained only by assuming hybridization of Cu *d* states, so that these states contribute to the lower valence band in order to fill the two extra states.

Experimental XPS spectra have been interpreted as showing Cu^{+} and Se^{-} oxidation states (Fowlmer & Jellinek, 1980). This picture of the charge transfer in hexagonal CuSe is qualitatively confirmed by the results of the Mulliken population analysis. Mulliken charges and bond populations calculated for the plane-wave basis formalism according to the scheme suggested by Segall *et al.* (1996) provide only a qualitative picture, especially for a metallic system that cannot be naturally represented using the localized atomic-like basis set. Nevertheless, the changes in calculated atomic charges and bond populations faithfully reproduce the changes in the nature of interatomic bonding. In particular, it has been shown that Mulliken charges and bond populations can be used to analyse pressure-induced structural phase transitions in solids (Winkler *et al.*, 2001).

The pressure dependence of the atomic charges and bond populations is shown in Figs. 9 and 10, respectively. The charge transfer is quite small, of the order of 0.1–0.2 electron per atom. This result differs from the experimental finding by Fowlmer & Jellinek (1980) of the Cu and Se valence states as +1 and −1, respectively, for two reasons:

(i) Mulliken charges only give a qualitative picture of the atomic charges, especially in metallic systems;

(ii) XPS does not produce accurate atomic charges either and the data are always open to interpretation.

Charge transfer and bond strength are found to be higher in the hexagonal layer than in the tetrahedral layer. The amount of charge transfer decreases under pressure, although the charge state of Cu1 atoms hardly changes up to 60 GPa (Fig. 9). The bond strength increases under pressure within both hexagonal and tetrahedral layers, Fig. 10. The increased amount of electron density in the Cu1—Se1 and Cu2—Se2 bonds causes weakening of the longer Cu2—Se1 bonds that hold the two types of layers together. The pressure of 60 GPa that corresponds to a complete structural reconstruction reduces the Cu2—Se1 bond strength of zero. This agrees with the structural changes described above, *i.e.* the bonding between the sheets is now achieved *via* the creation of the Se1—Se2 bonds and effectively breaking up the Se2—Se2 dumbbells. Indeed, the Se2—Se2 pairs show antibonding electronic states above 60 GPa according to the results of the Mulliken analysis, see Fig. 10.

The driving force for the instability of the hexagonal phase has been discussed in the literature in the context of the temperature-induced phase transitions. It has been suggested

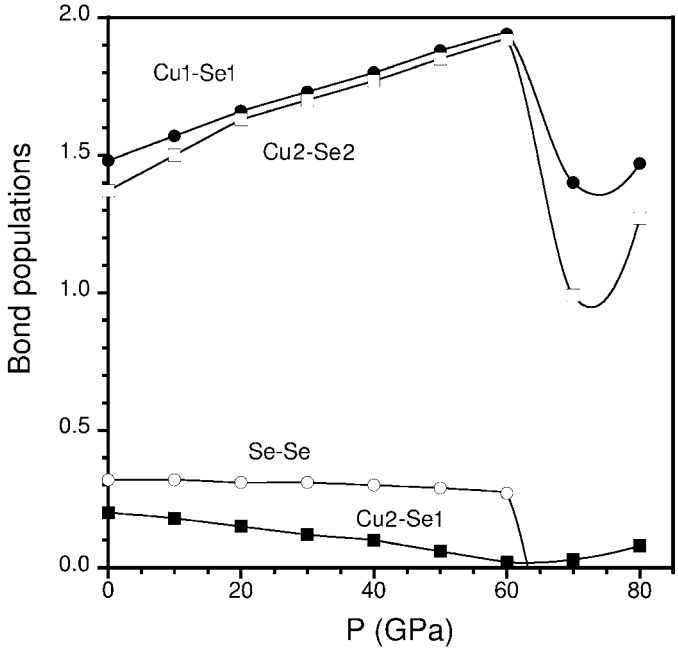

Figure 10
Pressure dependence of bond populations in hexagonal CuSe.

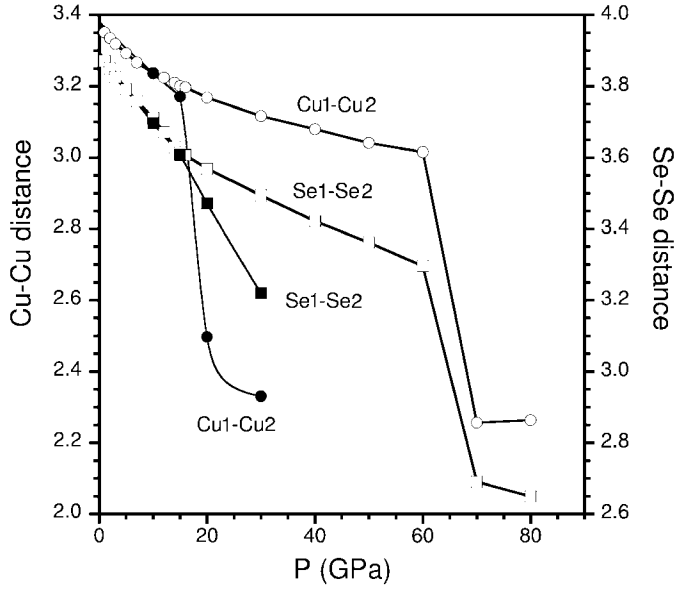

Figure 11
Pressure dependence of interatomic distances between nonbonded Cu1—Cu2 and Se1—Se2 atoms. Open symbols: calculations in the $P6_3/mmc$ space group; solid symbols: $P1$ space group.

Table 3
Theoretical and experimental bulk modulus and its pressure derivative for various phases of copper selenide.

Experimental data (Peiris *et al.*, 1998) are tentatively assigned to the low-temperature α-CuSe modification. The last line refers to my fitting of the experimental data (see text for an explanation).

Material	B (GPa)	B'
α-CuSe[(a)]	69 (2)	5.1 (5)
β-CuSe[(a)]	75 (1)	3.3 (1)
γ-CuSe[(a)]	72 (1)	4.6 (1)
Krutaite[(a)]	42 (6)	7 (1)
Umangite[(a)]	85 (2)	4.7 (4)
Exp.[(b)]	97 (5)	4.1 (5)
Exp. revisited[(c)]	72 (1)	4.6 (1)

References: (*a*) present results; (*b*) Peiris *et al.* (1998); (*c*) based on the data from Peiris *et al.* (1998).

that the shortening of the Cu1—Cu2 distances and to some extent of the Se1—Se2 distances could be responsible for the transition (Stølen *et al.*, 1996). According to the present results, the Se1—Se2 distances are slightly more affected by the pressure than the Cu1—Cu2 distances. This conclusion changes if one allows for the symmetry reduction in the calculations (Fig. 11). Without the symmetry restrictions imposed by the hexagonal $P6_3/mmc$ space group there is a dramatic shortening of the Cu1—Cu2 distances at 15 GPa. This finding agrees with the above-stated role of the Cu—Cu bonds in the transition. A complete description of the results obtained in the $P1$ space group will be given below.

Further analysis of the structural changes under pressure, Figs. 3–5, shows that there are obvious precursor events at pressures much lower than 60 GPa. The most pronounced feature can be observed at 15 GPa: there is a small plateau followed by the change of slope on the pressure dependence of the c/a ratio; a kink in the pressure dependence of the fractional coordinates, especially for Se_z; consequently, there are kinks on all the curves that describe the pressure dependence of interatomic distances. In addition, there are smaller changes at 7–8 GPa that lead, for example, to a non-monotonic pressure dependence of the bond length of the Se—Se dumbbells.

In summary, the hexagonal structure definitely loses stability at 60 GPa when the tetrahedral layer breaks down. The structure might transform at much lower pressures to a lower symmetry phase in order to introduce buckling of the flat hexagonal layer. The most likely pressure of such a transformation would be around 15 GPa, although even at lower pressures of 7–8 GPa there are already signs of structural instability.

3.2. Orthorhombic β-CuSe

The orthorhombic *Cmcm* structure is closely related to the hexagonal $P6_3/mmc$ one. The conventional cell of the ideal orthorhombic structure is obtained from the hexagonal cell by the transformation $\mathbf{a}' = 2\mathbf{a} + \mathbf{b}$. Conversely, the primitive cell of the *Cmcm* structure is very similar to the $P6_3/mmc$ cell, but the hexagonal angle is allowed to change. The degree of distortion of the orthorhombic cell is measured by the deviation of the $b/a3^{1/2}$ ratio from unity. The theoretical value of $b/a3^{1/2} = 1.009$ at $P = 0$ agrees well with the experimental estimates that range from 1.014 to 1.017 (Table 2).

The EOS parameters for β-CuSe, as determined from calculations at pressures up to 20 GPa, are $B = 75$ (1) GPa and $B' = 3.3$ (1). The bulk modulus is close to the one for the hexagonal modification, which is understandable in view of the close similarity of the two structures.

The orthorhombic structure differs from the hexagonal one in that there are two sets of the symmetry-unrelated Cu1—Cu2 and Se1—Se2 distances. This appears to be an important fact since these interactions might be responsible for the phase transitions in the CuSe system. The short Cu1—Cu2 distance in the orthorhombic cell is found to be shorter than the corresponding distance in the hexagonal cell at the same pressure. One thus expects Cu—Cu bonds to form at lower pressure than in the $P6_3/mmc$ structure. The short Cu1—Cu2 distance in the *Cmcm* structure is 3.135 Å at $P = 0$, which is very close to the value in the $P6_3/mmc$ cell at 15 GPa, the suggested instability point. These observations confirm the importance of the Cu—Cu interactions for the structural stability of klockmannite.

3.3. Hexagonal α-CuSe

The actual structure of the low-temperature hexagonal modification of CuSe is still unknown, as discussed in §1. An *ab initio* study reported below is based on the fully ordered $P6_3/m$ structure with $Z = 78$ suggested by Lippmann (1962). Note that the first-principles study of various disordered structures put forward in order to explain the diffraction patterns (Darlow, 1969; Von Effenberger & Pertlik, 1981) is extremely expensive and for practical purposes unrealistic.

The calculated cell parameters of the ground state of the ordered α-CuSe modification (Table 1) agree with the experimental data and are very close to the theoretical results for the simpler $P6_3/mmc$ hexagonal structure of γ-CuSe. There are inequivalent Cu1—Se1 bonds in the hexagonal layer in the α-CuSe structure in contrast with the γ-CuSe modification, with the bond lengths ranging from 2.280 to 2.300 Å. A similar scatter exists for the lengths of the inequivalent Cu2—Se2 bonds in the buckled tetrahedral layer, from 2.389 to 2.406 Å. The lengths of the Cu2—Se1 bonds that keep the layers together range from 2.460 to 2.471 Å and the Se—Se dumbbell bonds are from 2.373 to 2.399 Å. A quick comparison of these numbers to the results for γ-CuSe presented in Fig. 5 shows that the values quoted above are scattered around the bond-length values in the $P6_3/mmc$ structure.

The difference between the $Z = 78$ structure and the $P6_3/mmc$ one is fairly small. In fact, the symmetry analysis of the calculated α-CuSe structure with the moderate tolerance of 0.4 Å reports the symmetry as $P6_3/mmc$ with $Cu_z = 0.1125$ and $Se_z = 0.0666$. The energies of the two structures are also very similar, as will be discussed below.

The optimized α-CuSe structure was used to re-examine the mismatch between the tetrahedron side length and the

Table 4
Experimental and theoretical structure of umangite, Cu_3Se_2.

a (Å)	c (Å)	Cu (4e)	Se (4e)
6.394 (5)[(a)]	4.269 (5)[(a)]	–	–
6.405[(b)]	4.278[(b)]	–	–
6.385[(c)]	4.271[(c)]	–	–
6.402 (1)[(d)]	4.279 (1)[(d)]	0.647 (5), 0.853 (5), 0.219 (5)	0.272 (3), 0.772 (3), 0.264 (7)
6.406 (2)[(e)]	4.279 (2)[(e)]	0.647, 0.853, 0.250	0.275, 0.225, 0.250
6.308[(f)]	4.350[(f)]	0.6430, 0.8570, 0.2475	0.2655, 0.7655, 0.2586

References: (*a*) Heyding (1966); (*b*) Stevels (1969) and Stevels & Jellinek (1971); (*c*) Murray & Heyding (1975); (*d*) Heyding & Murray (1976); (*e*) Morimoto & Koto (1966); (*f*) present results.

triangle side length (Lippmann, 1962). The optimized γ-CuSe has the tetrahedra with side length 3.893 Å, as determined by the Cu2—Se2 distance, while the Se1—Se1 triangles in the flat layer have side lengths 3.973 Å. The lowering of symmetry in the α-CuSe structure produces a variety of slightly different side lengths in both layers. The hexagonal layer is largely unchanged and one can still use the value of 3.973 Å as the representative length of the triangle side. The tetrahedra distort much stronger and they exhibit the scatter of the side lengths from 3.866 to 3.939 Å. The longest of these distances obviously match the dimensions of the triangular layer more closely than in the γ-CuSe structure, in agreement with the hypothesis put forward by Lippmann (1962).

One can expect that the low-temperature α-CuSe modification might be more compressible than the γ-CuSe structure, since it has noticeably more degrees of freedom to accommodate the deformation. The present calculation predicts only minor softening – the bulk modulus B is obtained as 69 (2) GPa, and B' = 5.1 (5). Table 3 shows that the compressibility of all three studied polymorphs is very similar,

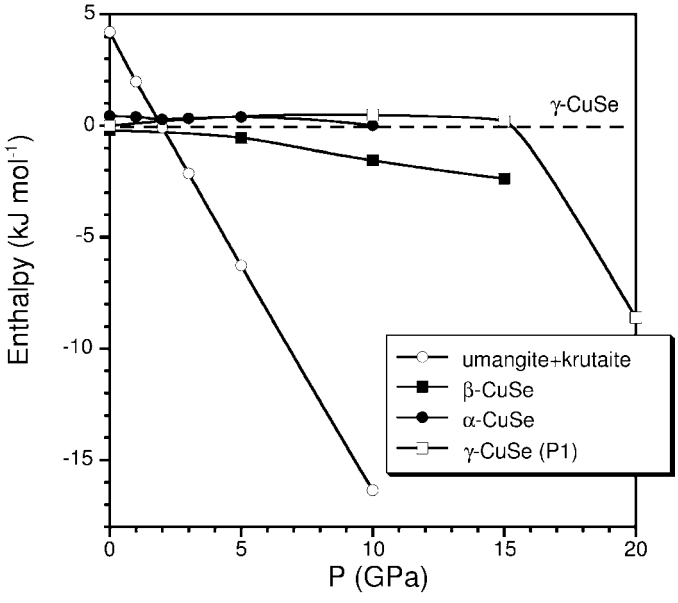

Figure 12
Pressure dependence of the enthalpy of various phases of copper selenide relative to the enthalpy of the hexagonal $P6_3/mmc$ γ-CuSe.

which can be understood in terms of structural similarities between these modifications of CuSe.

3.4. Klockmannite in *P*1 space group

All the calculations described above were carried out under the symmetry constraints imposed by the corresponding space groups. The results presented in this section do not assume *a priori* any symmetry in the system. They were obtained by introducing small random displacements for all atoms in the $P1$ setting for the corresponding polymorph. Symmetry analysis was performed on all structures obtained after geometry optimization of the randomized $P1$ systems. Finally, these calculations were repeated with increased supercells (*e.g.* Z = 12 instead of Z = 6 for γ-CuSe).

Hexagonal CuSe in the $P1$ setting converges to essentially the same structure as in the original runs in the $P6_3/mmc$ space group for pressures between 0 and 15 GPa. By specifying very strict criteria in symmetry analysis, the orthorhombic *Cmcm* symmetry is recovered at P = 0 GPa. The degree of orthorhombic distortion found in this case is very small, at least three times below the value for the constrained runs on *Cmcm* structure reported in the previous sections. At higher pressures the symmetry is determined as at best $P2_1$. Removal of symmetry constraints in these calculations allows much stronger deformation of the hexagonal sheets, which facilitates the formation of the Cu1—Cu2 bonds, see Fig. 11.

It is conceivable that the original Z = 6 cell for the hexagonal modification is so small that it is not possible to obtain more complex structures using it as a starting point. However, the calculation with $P1$ symmetry using a bigger cell with the doubled period along the b axis also converged to the $P6_3/mmc$ hexagonal structure. The doubled cell showed greater distortions of the structure and shorter Cu—Cu distances upon compression compared with single-cell calculations. It appears that the more variational freedom the system has, the more likely the Cu—Cu bond formation under pressure.

The calculations based on the $P1$ version of the *Cmcm* orthorhombic structure for pressures up to 20 GPa produce the structure that can only be interpreted as *Cmcm* in the symmetry analysis. Once again, the main difference compared with the symmetry-constrained calculations is that the Cu—Cu distance decreases much more rapidly under pressure.

3.5. Krutaite, $CuSe_2$ II

Krutaite is one of the modifications of $CuSe_2$. It crystallizes in the cubic structure of the pyrite type, space group $Pa\bar{3}$ (Z = 4). Cu atoms are on the Wyckoff positions 4(a) with coordinates (0, 0, 0) and Se atoms are on the 8(c) Wyckoff positions with coordinates (x, x, x). The experimental lattice parameter of krutaite is 6.116 (1) Å and the only internal degree of freedom is Se_x = 0.3891 (5) (Heyding & Murray, 1976). Magnetic effects were neglected in the calculations as krutaite is reported to be an exceedingly weak ferromagnet at low temperatures (Kontani *et al.*, 2000). The calculated ground state for this structure is characterized by a = 6.119 Å and

Se_x = 0.3904, in good agreement with the experimental data. Krutaite is found here to have B = 42 GPa, so it is noticeably softer than other CuSe polymorphs (Table 3).

Mulliken charges on all atoms in the krutaite structure are much smaller than in klockmannite, +0.06 on Cu and −0.03 on Se. Se—Se is the strongest bond in the structure – it is slightly shorter than the Se—Se dumbbell bond in klockmannite (2.32 Å compared with 2.39 Å), and the Mulliken bond population is 0.41 compared with 0.31. The Cu—Se bonds are 2.57 Å long, significantly longer than any of the Cu—Se bonds in CuSe. They are consequently much weaker, with bond populations of only 0.22.

3.6. Umangite, Cu_3Se_2

Umangite has a tetragonal structure, space group $P\bar{4}2_1m$ (Z = 2). Cu atoms are located on the Wyckoff positions 2(a) (0, 0, 0) and on the general positions 4(e) with coordinates (x, y, z), and all Se atoms are on the general positions 4(e). The calculated lattice parameters of a = 6.308, c = 4.350 Å and the internal coordinates of Cu and Se atoms on the general positions are in reasonable agreement with the reported experimental values (see Table 4). Umangite is found to have the highest bulk modulus, 85 GPa, of all other copper selenide phases studied here (Table 3).

Bonding in umangite is characterized by a stronger charge transfer than in krutaite and a more covalent character of Cu—Se bonds. Mulliken charges are found to be −0.17 on Se, and +0.09 and +0.13 on two inequivalent Cu atoms. Cu—Se bonds are shorter than in krutaite, 2.42–2.52 Å. Mulliken bond populations for the shortest bonds are as high as 0.83, which is comparable to Cu—Se bond populations in klockmannite (Fig. 10).

4. Energetics of CuSe under pressure

The results presented in the previous sections can be used to analyse the phase stability of copper selenide under compression. The summary of the available data is presented in Fig. 12, where the enthalpies are shown relative to the hexagonal γ-CuSe. A number of conclusions can be made based on these results.

The orthorhombic β-CuSe is shown to be marginally more stable than the hexagonal γ-CuSe at zero pressure. The energy difference of 0.2 kJ mol^{-1} is significantly below the confidence level of the present calculations. It is possible that the ordering of energies at P = 0 would be reversed if thermal effects were taken into account. The same comment is valid for the complex structure of α-CuSe, which is found to be 0.4 kJ mol^{-1} less stable than γ-CuSe.

The orthorhombic β-CuSe becomes the most stable polymorph under compression. This might correspond to the experimentally observed transition from γ-CuSe to β-CuSe on cooling, which is in some ways analogous to applying external pressure. The enthalpy differences between different CuSe phases are of the same order as reported experimentally (*e.g.* 0.855 kJ mol^{-1} for the γ- to β-CuSe transition as determined by Stølen *et al.*, 1996).

The structure proposed by Lippmann (1962) for the low-temperature α-CuSe phase is characterized by essentially the same $H(P)$ dependence as a much simpler hexagonal γ-CuSe polymorph. It is thus possible that the true low-temperature phase is disordered and non-stoichiometric, as was suggested earlier.

The most striking result comes from the comparison of the stability of CuSe polymorphs to that of the mixture of krutaite, $CuSe_2$, and umangite, Cu_3Se_2. The $H(P)$ dependence for this mixture has a different slope from that of all the CuSe phases and thus it is possible to determine the phase transition point unambiguously. It appears that at 2 GPa the mixture of krutaite and umangite becomes more stable and thus the disproportionation of klockmannite is expected. This transition pressure of 2 GPa at zero temperature is to be compared to the experimentally reported 1 GPa disproportionation pressure at room temperature (Murray & Heyding, 1975). DFT calculations cannot be expected to produce transition pressures with greater accuracy than 1 GPa (Milman *et al.*, 2000; Milman, 1997; Winkler *et al.*, 2001) and thus one has to conclude that theory and experiment are in good agreement for the value of the transition pressure.

This conclusion is relevant to the experimental study of the equation of state of klockmannite (Peiris *et al.*, 1998). It follows from Fig. 12 that regardless of the nature of the stable CuSe phase at P = 0 (α-, β- or γ-CuSe) it transforms to the mixture of krutaite and umangite under pressure. Experiment suggests that this is a rapid transition at room temperature (Murray & Heyding, 1975). If this is the case, the EOS results reported by Peiris *et al.* (1998) refer to a mixture of copper selenide compounds and are not representative of klockmannite. Low-temperature high-pressure studies would be required to determine the compressibility of CuSe itself, as disproportionation should become inhibited on cooling.

4.1. Bulk modulus of klockmannite

The apparent discrepancy between the calculated, 72 GPa, and measured, 97 GPa (Peiris *et al.*, 1998), values of the bulk modulus of hexagonal CuSe warrants a separate investigation. The experimental and theoretical data for γ-CuSe are in good agreement over the complete pressure range of the experimental study, 0–52 GPa (Fig. 2). It is unusual to have a 25% deviation in bulk modulus values when the P–V data agree so well. DFT is known to reproduce the compressibility of inorganic solids to at least 10% (Milman *et al.*, 2000) and the magnitude of the discrepancy observed here is thus puzzling.

It is conceivable that a certain amount of a less compressible compound umangite was present in the experiment as a result of the pressure-induced disproportionation. It is difficult to explain the discrepancy by this hypothesis alone, as a much softer compound krutaite would be introduced at the same time.

Since the experimental study by Peiris *et al.* (1998) was carried out at room temperature the results should correspond

to the α-phase rather than to the γ-phase. However, theoretical results suggest that the bulk modulus of all CuSe structures is very similar (Table 3).

Finally, the EOS fitting procedure with a third-order Birch–Murnaghan equation of state, as described above for the theoretical EOS calculations, was applied to the raw P–V data reported by Peiris *et al.* (1998). The fitting over the full range of this data produced B = 72 (1) GPa and B' = 4.6 (1) as opposed to the values reported by Peiris *et al.* (1998), B = 97 (5) GPa and B' = 4.1 (5). These new values are in excellent agreement with the theoretical estimates, as one would expect from the visual inspection of the two sets of P–V data reported in Fig. 2.

5. Conclusions

The first *ab initio* study of the structural and electronic properties of the three different polymorphs of CuSe at ambient conditions and under high pressures is presented. The results indicate a number of possible pressure-induced instabilities in the hexagonal γ-CuSe, most notably at 15 GPa. These instabilities might be responsible for metastable phases reported in high-temperature–high-pressure studies (Von Effenberger & Pertlik, 1981; Nozaki *et al.*, 1995).

The ordered structure of a more complex hexagonal polymorph with 156 atoms in the unit cell, α-CuSe (Lippmann, 1962), has been studied in detail for the first time. It is shown that its properties are very similar to those of the γ-CuSe polymorph and thus the possibility of a completely different disordered structure of low-temperature polymorph cannot be ruled out.

A comparison of trends predicted in the behaviour of klockmannite under pressure to the experimental results related to temperature-induced phase transitions suggests that a hexagonal phase transforms to the orthorhombic structure under pressure. The driving force for the transition is the same as in the γ-CuSe to β-CuSe transition observed on cooling (Fjellvåg *et al.*, 1988; Stølen *et al.*, 1996), namely, the Cu–Cu contacts between hexagonal and tetrahedral layers lead to the formation of Cu—Cu bonds.

The experimentally observed disproportionation of klockmannite into krutaite and umangite is explained on the basis of the calculated pressure dependence of the enthalpies for various phases of copper selenide. The calculated pressure of this transition is in good agreement with the existing experimental observations (Murray & Heyding, 1975).

The bulk modulus was calculated for all the compounds studied. The experimentally reported value of 97 GPa (Peiris *et al.*, 1998) is shown to be in error and the actual bulk modulus of CuSe is suggested to be around 70 GPa.

I am grateful to Nic Austin for bringing the subject of this paper to my attention and to Bjoern Winkler for numerous discussions of the effects of pressure on solids. Calculations for α-CuSe were carried out on an IBM *RS*/6000 SP operated by the Center for Computational Sciences of Oak Ridge National Laboratory, which is supported by the Office of Science of the US Department of Energy under Contract No. DE-AC05-00OR22725.

References

Accelrys Inc. (2001). *CASTEP User's Guide.* Accelrys Inc., San Diego, CA.
Berry, L. G. (1954). *Am. Mineral.* **39**, 504–509.
Birch, F. (1978). *J. Geophys. Res.* **83**, 1257–1268.
Brun, G., Tedenac, J. C. & Maurin, M. (1982). *Mater. Res. Bull.* **17**, 379–382.
Darlow, S. F. (1969). *Acta Cryst.* A**25**, S109.
De Vita, A. (1992). PhD Thesis. Keele University, England.
Earley, J. W. (1949). *Am. Mineral.* **34**, 435–440.
Elliott, J. A., Bicknell, J. A. & Collinge, R. G. (1969). *Acta Cryst.* B**25**, 2420.
Fischer, T. H. & Almlöf, J. (1992). *J. Phys. Chem.* **96**, 9768–9774.
Fjellvåg, H., Grønvold, F., Stølen, S., Andresen, A. F., Müller-Käfer, R. & Simon, A. (1988). *Z. Kristallogr.* **184**, 111–121.
Fowlmer, J. C. W. & Jellinek, F. (1980). *J. Less-Common Met.* **76**, 153–162.
Heyding, R. D. (1966). *Can. J. Chem.* **44**, 1233–1236.
Heyding, R. D. & Murray, R. M. (1976). *Can. J. Chem.* **54**, 841–848.
Hohenberg, P. & Kohn, W. (1964). *Phys. Rev.* **136**, 864–871.
Kohn, W. & Sham, L. J. (1965). *Phys. Rev. A*, **140**, 1133–1138.
Kontani, M., Tutui, T., Moriwaka, T. & Mizukoshi, T. (2000). *Physica B*, **284–288**, 675–676.
Kresse, G. & Furthmüller, J. (1996). *Phys. Rev. B*, **54**, 11169–11186.
Lippmann, F. (1962). *Neues Jahrb. Mineral. Monatsh.* pp. 99–105.
Milman, V. (1997). *Properties of Complex Inorganic Solids*, edited by A. Gonis, A. Meike & P. E. A. Turchi, pp. 19–24. Plenum Press: New York.
Milman, V., Winkler, B., White, J. A., Pickard, C. J., Payne, M. C., Akhmatskaya, E. V. & Nobes, R. H. (2000). *Int. J. Quant. Chem.* **77**, 895–910.
Monkhorst, H. J. & Pack, J. D. (1976). *Phys. Rev. B*, **13**, 5188–5192.
Morimoto, N. & Koto, K. (1966). *Science*, **152**, 345–346.
Murray, R. M. & Heyding, R. D. (1975). *Can. J. Chem.* **53**, 878–887.
Nozaki, H., Shibata, K., Ishii, M. & Yukino, K. (1995). *J. Solid State Chem.* **118**, 176–179.
Nozaki, H., Shibata, K., Onoda, M., Yukino, K. & Ishii, M. (1994). *Mater. Res. Bull.* **29**, 203–211.
Payne, M. C., Teter, M. P., Allan, D. C., Arias, T. A. & Joannopoulos, J. D. (1992). *Rev. Mod. Phys.* **64**, 1045–1097.
Peiris, S. M., Pearson, T. T. & Heinz, D. L. (1998). *J. Chem. Phys.* **109**, 634–636.
Perdew, J. P., Chevary, J. A., Vosko, S. H., Jackson, K. A., Pederson, M. R., Singh, D. J. & Fiolhais, C. (1992). *Phys. Rev. B*, **46**, 6671–6687.
Segall, M. D., Pickard, C. J., Shah, R. & Payne, M. C. (1996). *Phys. Rev. B*, **54**, 16317–16320.
Stevels, A. L. N. (1969). *Philips Res. Repts.* Suppl. No. 9.
Stevels, A. L. N. & Jellinek, F. (1971). *Rec. Trav. Chim. Pays-Bas*, **111**, 273–283.
Stølen, S., Fjellvåg, H., Grønvold, F., Sipowska, J. & Westrum, E. F. Jr (1996). *J. Chem. Thermodyn.* **28**, 753–766.
Taylor, C. A. & Underwood, F. A. (1960). *Acta Cryst.* **13**, 361–362.
Vanderbilt, D. (1990). *Phys. Rev. B*, **41**, 7892–7895.
Von Effenberger, H. & Pertlik, F. (1981). *Neues Jahrb. Mineral. Monatsh.* pp. 197–205.
White, J. A. & Bird, D. M. (1994). *Phys. Rev. B*, **50**, 4954–4957.
Winkler, B. & Milman, V. (1997). *J. Phys. Condens. Matter*, **9**, 9811–9817.
Winkler, B., Pickard, C. J. & Milman, V. (2001). *Phys. Rev. B* **63**, 214103.